Supporting Information for
Observation of one-dimensional Dirac fermions in silicon nanoribbons

Shaosheng Yue,[1,5] Hui Zhou,[1,5] Ya Feng,[2] Yue Wang,[3] Zhenyu Sun,[1,5] Daiyu Geng,[1,5] Masashi Arita,[4] Shiv Kumar,[4] Kenya Shimada,[4] Peng Cheng,[1,5] Lan Chen,[1,5,6] Yugui Yao,[3] Sheng Meng,[1,5] Kehui Wu,[1,5,6] and Baojie Feng[1,5]

[1]*Institute of Physics, Chinese Academy of Sciences, Beijing 100190, China*
[2]*Beijing Academy of Quantum Information Sciences, Beijing 100193, China*
[3]*Key Lab of Advanced Optoelectronic Quantum Architecture and Measurement (MOE), Beijing Key Lab of Nanophotonics Ultrafine Optoelectronic Systems, and School of Physics, Beijing Institute of Technology, Beijing 100081, China*
[4]*Hiroshima Synchrotron Radiation Center, Hiroshima University, 2-313 Kagamiyama, Higashi-Hiroshima 739-0046, Japan*
[5]*School of Physical Sciences, University of Chinese Academy of Sciences, Beijing 100049, China*
[6]*Songshan Lake Materials Laboratory, Dongguan, Guangdong 523808, China*

(Dated:)

1. Topological Phase Transition in the Presence of Magnetic Field

When time-reversal symmetry is broken, the 1D Dirac cone will split into a pair of Weyl cones, as marked by 1 in Fig. S1, which can be realized by applying a uniform magnetic field. Each Weyl cone can be described by a single-spin SSH model. With weak magnetic field, this pair of Weyl cones will cross each other and form another pair of Weyl cones, as indicated by 2 in Fig. S1. This pair of Weyl cones are protected by the U(1) symmetry since the two crossing bands have opposite spin indexes. Therefore, the second pair of Weyl cones cannot be gapped by spatial perturbations. However, this pair of Weyl cones will be gapped when spin-orbit coupling effects are taken into account.

In conclusion, we predict that the 1D Dirac cone in SiNRs will split into two pairs of 1D Weyl cones. One pair split in the energy direction and each Weyl cone can be described by a single-spin SSH model; the other pair split in the momentum direction and is protected by the U(1) symmetry. The rich physics in the momentum direction calls for further experimental and theoretical investigations.

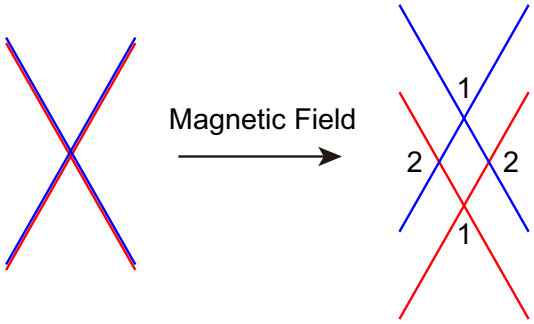

FIG. S1: Schematic drawing of the topological phase transition in the magnetic field. The red and blue lines indicate spin up and spin down, respectively. The 1D Dirac cone split into two pairs of 1D Weyl cones.

2. Scanning Tunneling Spectroscopy (STS) Measurements

The dI/dV spectra of SiNRs are shown in Fig. S2. We observe a dip feature at ∼0.8 eV below the Fermi level, as indicated by the black arrow. This dip corresponds to the Dirac point of SiNRs, which agrees well with our ARPES results.

3. Band structures of Ag(110)

An ARPES intensity map of the Fermi surface of pristine Ag(110) are shown in Figs. S3(a). The pocket at the $\bar{Y}$ point corresponds to the Shockley surface states of silver. The other bands derive from the bulk states of Ag(110), as indicated by "BS". Figures S3(b) and S3(c) shows the calculated bulk *sp* band of Ag, which qualitatively agree with our experimental results.

4. Orbital Resolved Band structures of SiNRs on Ag(110)

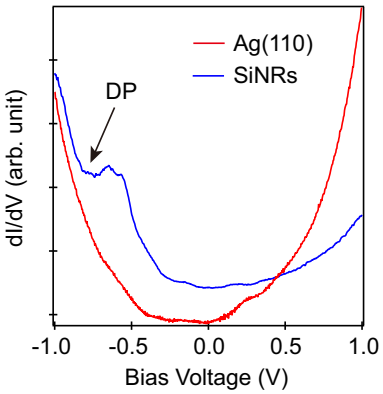

FIG. S2: dI/dV spectra of SiNRs (blue) and bare Ag(110) (red), respectively. The dip at E_B ~0.8 eV corresponds to the Dirac point (DP), as indicated by the black arrow. Tunneling current: 0.3 nA.

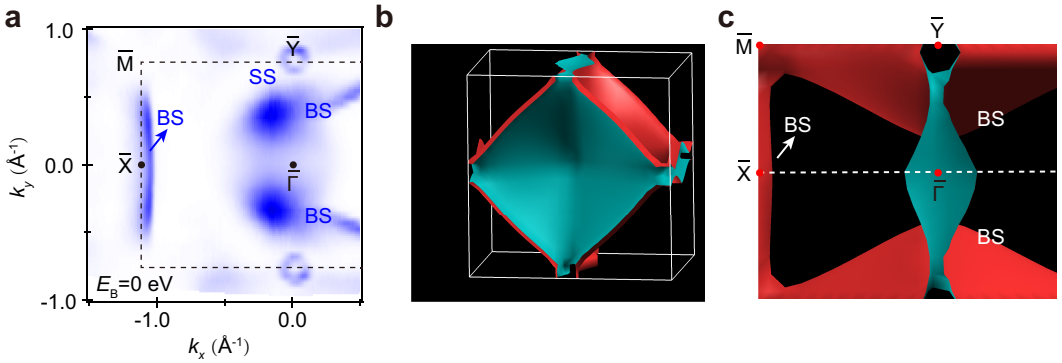

FIG. S3: a) ARPES intensity map of the Fermi surface of pristine Ag(110) measured with 35-eV photons. The wave vector and polarization of the incident light are coplanar with the $\bar{\Gamma}$–$\bar{X}$ line. (b) Calculated Fermi surface of the bulk *sp* band in the 3D Brillouin zone of bulk Ag. (c) Calculated Fermi surface of the bulk *sp* band viewed from the (110) surface.

To clarify the origin of the 1D Dirac bands in SiNRs/Ag(110), we projected the unfolding band structures of SiNRs/Ag(110) to different atomic layers, as shown in Figs. S4(a)-S4(d). One can see that the Dirac bands are mainly localized at the surface Si layer, with only a small amount of remanent signal at the topmost Ag layer. The remanent signal in the topmost Ag layer indicates finite band hybridization between Si and Ag. The 8th Ag layer only contain the bulk bands of Ag(110), as shown in Fig. S4(c). By comparing Figs. S4(a) and S4(c), we can also conclude that the bands with strong intensity near the Dirac bands derive from the bulk of Ag(110). In fact, these bands derive from the subbands of Ag bulk *sp* bands because of the slab geometry in our calculation. To study the orbital composition of the Dirac bands, we projected the unfolding band structures to different orbitals of Si_s and Si_{ad} atoms, as shown in Figs. S4(e)-S4(l) and found that the Dirac bands are dominated by Si_s p_z orbitals. These results agree with our TB analysis that the p_z orbitals of Si_s and Si_{ad} atoms are decoupled.

5. First-Principles Calculation Results of Double-Strand SiNRs on Ag(110)

Figure S5 shows the first-principles calculation results of double-strand SiNRs on Ag(110). Overall, the calculated band structures of double-strand SiNRs are similar to those of single-strand SiNRs. The slight difference originates from the coupling between adjacent SiNRs.

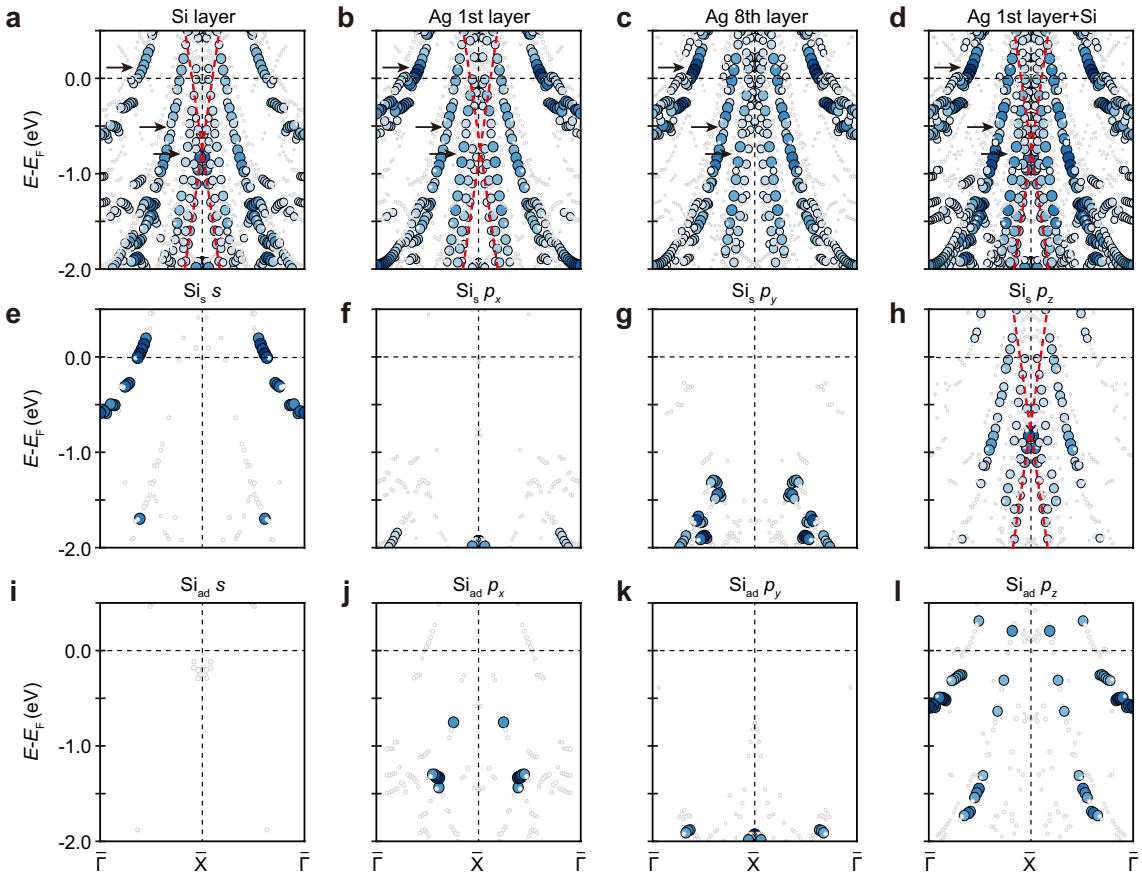

FIG. S4: (a)-(d) Calculated band structures along the $\bar{\Gamma}$–$\bar{X}$–$\bar{\Gamma}$ direction projected to the Si layer, Ag 1st (topmost) layer, Ag 8th layer, and both the Si layer and Ag 1st layer, respectively. The black arrows indicate the bulk bands of Ag(110) because the spectral weights of these bands are higher at deeper Ag layers. (e)-(h) Calculated band structures projected to Si$_s$ s, p_x, p_y, and p_z orbitals, respectively. (i)-(l) Calculated band structures projected to Si$_{ad}$ s, p_x, p_y, and p_z orbitals, respectively. The Dirac bands are indicated by red dashed lines in (a), (d) and (h).

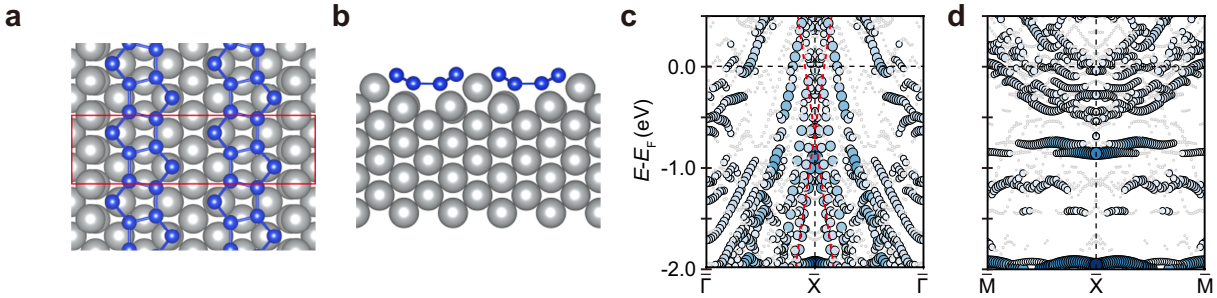

FIG. S5: (a) and (b) are top view and side view of double-strand SiNRs on Ag(110). Blue and gray balls represent Si and Ag atoms, respectively. The red rectangle in (a) indicates a unit cell. (c) and (d) DFT calculated band structure projected to nanoribbon and topmost Ag layer along $\bar{\Gamma}$–$\bar{X}$–$\bar{\Gamma}$ and $\bar{M}$–$\bar{X}$–$\bar{M}$, respectively. The band structure is unfolded to the first Brillouin zone of Ag(110).